



Original article

Evaluation of inter-individual pelvic CT-scans registration

Évaluation de recalage inter-individus de tomodensitométries pelviennes

G. Dréan^{a,*,b}, O. Acosta^{a,b}, A. Simon^{a,b}, R. de Crevoisier^{a,b,c}, P. Haigron^{a,b}

^a LTSI, université de Rennes 1, campus de Beaulieu, bâtiment 22, 35000 Rennes, France

^b Inserm U642, campus de Beaulieu, bâtiment 22, 35000 Rennes, France

^c Département de radiothérapie, centre Eugène-Marquis, Rennes, France

Received 19 July 2011; received in revised form 29 August 2011; accepted 29 August 2011

Abstract

Image registration appears to be an essential tool in a wide range of biomedical applications. We are interested in performing voxel-wise population analysis aimed at explaining sideways effects of dose irradiation across a population treated for prostate cancer. To this end, a perfect registration of pelvic computed tomography (CT) scans is required allowing a reliable mapping of dose distributions in a single coordinate system. In this paper, we compared the performances of four different inter-individual intensity-based registration strategies: two affine (block matching and mask-restricted block matching) and two non-rigid (diffeomorphic demons and free-form deformation). Pelvic CT-scans were registered towards a single template in a leave-one-out cross validation scheme. The ability of the methods to align inter-individual images was assessed in terms of overlap measures between the manually segmented organs after the registration. Results show that the free-form deformation registration strategy outperformed the other methods and provided more accurate registrations. We showed that precision can be improved by restricting the algorithm calculations to the main regions of interest.

© 2011 Elsevier Masson SAS. All rights reserved.

1. Introduction

Image registration is a cornerstone in many biomedical applications where the challenge lies in finding spatial correspondences between various image time-modality series. Registration allows comparisons either for detecting changes in time across a population, or for enriching the information provided by different modalities. Examples of registration may be found at the core of surgical guidance procedures [1], in individual's follow-up while performing a therapy [2], in population analysis [3], in multimodal-fusion [4,5], in template-building problems [6], or within a segmentation framework [7], such as atlas-based segmentation [8,9].

A wide range of registration methods have been proposed for medical images [10]. A key point shared by all of them is the computation of a spatial transformation (rigid, affine, non-rigid) mapping a moving image to a fixed one by optimizing a similarity criteria. The similarity may be based on control points,

visible features, anatomical structures, or image intensities. In this paper, we are mainly interested in intensity-based metrics and in two types of transformations, namely affine and non-rigid. The motivation of this work is to further perform voxel-wise population analysis in the context of prostate cancer radiotherapy [14]. In this context, the inter-individual organ alignment is of up-most importance in order to be able to compare dose distributions across a population. Recent works already performed voxel-wise analysis and compared prescribed dose with toxicity outcomes in the urinary tract [22] and with tumor control in the prostate [23]. However, those methods are approximated in terms of spatial location as the mapping was defined by a parametric representation of the whole image with respect to the organs position in polar coordinates. As opposed to them, we aim to perform finer comparisons at a voxel level and thus to accurately register several individuals' pelvic computed tomography (CT) images towards a common coordinate system. This task is particularly challenging due to difficulties related to the poor soft tissue contrast in the CT-scans, the large inter-individual variability and the filling variability of the bladder and the rectum, as pointed out in [8].

* Corresponding author.

E-mail address: gael.drean@univ-rennes1.fr (G. Dréan).

A major challenge in registration is the validation as the ground truth may be hardly defined and it strongly depends on the clinical application and the data being used. Different approaches for registration validation may be found [2,10,12,13]. Some previous works have performed validation of pelvic CT-scans registration [15,16], but it was mainly done by comparing the registration results with a mathematically known transformation and no overlap between the organs was computed.

In this paper, we compared the performance of four intensity-based registration strategies, two affine and two non-rigid, in the alignment of inter-individual pelvic CT-scans within the scope of population analysis. Namely, block matching (BMA) [17] and mask-restricted block matching (RMA) affine registrations [17] and diffeomorphic demons [18,19] and free-form deformation (FFD) [20,21], non-rigid registrations. The performance was measured as the overlap between organ manual segmentations for prostate, bladder and rectum after registration, in a leave-one out cross validation scheme.

2. Patients and methods

2.1. Data

We carried out our study on a set of 24 prostate cancer patients, treated with external radiotherapy. Each individual underwent a planning CT-scan. All acquired CT-scans were 2 mm slice thickness with a 512×512 1 mm pixels resolution in the axial plan. For each individual, the organs were manually delineated by the same expert, following the standard clinical protocol in radiotherapy. The expert contoured the clinical target (prostate and seminal vesicles) and the organs at risk (OAR)

(the bladder and the rectum). In this study, only the CT-scans and the delineated prostate, bladder and rectum were considered (Fig. 1).

2.2. Registration strategies

Two intensity-based affine and two non-rigid registration strategies were combined as follows:

- “block matching” affine registration (BMA) [17]: This multi-resolution algorithm consists in taking a $N \times N$ size block in the moving image and then finding, in the fixed image, the same sized block with the highest similarity, in the sense of the normalized cross correlation (CC) (Eq.(1)). The global affine transformation is then estimated from these local matches as the solution of a robust regression problem. This algorithm was applied on the whole image;

$$CC = \frac{\sum(I - E(I))(A_N - E(A_N))}{\sqrt{(\sum_x(I - E(I)))^2} \sqrt{(\sum_x(A_N - E(A_N)))^2}} \quad (1)$$

- “block matching” restricted by mask affine registration (RMA) [17]: The principle of this method is the same as the one mentioned above, but rather than applying the algorithm on the whole image, we restricted the deformation computation by using a mask created from the segmentation of the individual's bodies with a 5 mm margin;
- non-rigid registration using the diffeomorphic demons algorithm (demons) [18,19]: This multi-resolution registration algorithm considers the images as series of contours on which control points are placed. To match the points between the moving and the fixed image, a set forces solving an optical

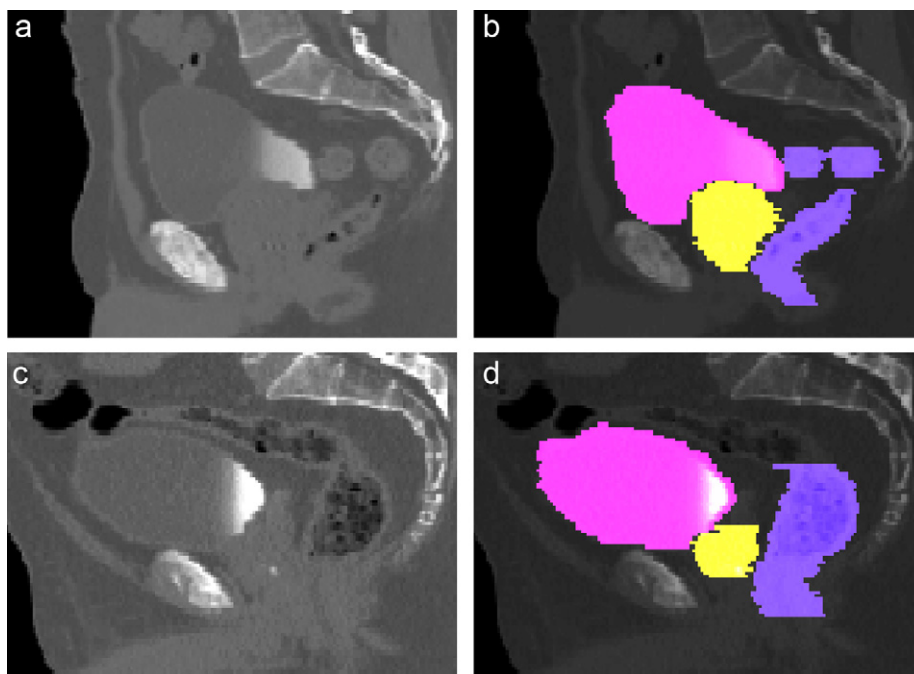


Fig. 1. Example of two computed tomography (CT) sagittal views (a and c) with the delineated organs (b and d): prostate (yellow), bladder (pink) and rectum (mauve).

flow problem are calculated (Eq.(2)). At each iteration, a regularization is done by applying a Gaussian filter to smooth and control the deformation field and prevent from excessive deformations.

$$T^{i+1} = \frac{2(T^i(I_S) - I_T) \left(\nabla T^i(I_S) + \nabla I_T \right)}{\left\| \nabla T^i(I_S) + \nabla I_T \right\|} \quad (2)$$

where T^i is the i^{th} displacement field, $T^i(I_S)$ the warped source image I_S and I_T the target image;

- non-rigid registration using the FFD algorithm [20,21]: The technique of the FFD is based on a multi-resolution cubic B-Splines calculation. After the calculation of the similarity measure (MI) (Eq.(3)), the transformation is defined on a grid of control points. Then, the transformation is applied on the control points and the regularization is computed by a B-Splines interpolation.

$$MI = H(I) + H(A_N) - H(I, A_N) \quad (3)$$

where $H(x)$ is the individual entropy of image, given by $H(x) = -\sum_x PX(x) \log PX(x)$ and $H(I, A_N) = -\sum_{a,b} pIA_N(a, b) \log pIA_N(a, b)$ is the joint entropy and pIA_N is the joint probability distributions of pixels associated with the images I et A_N .

The non-rigid diffeomorphic demons algorithm was combined to the BMA and then the non-rigid FFD algorithm to the RMA registration results.

2.3. Validation

We performed a leave-one-out cross validation in which each one of the 24 individuals' CT-scans was iteratively chosen as the common template. Using the computed transformation between each individual's CT and the template, the organs (prostate, bladder and rectum) were propagated using a *nearest neighbor* interpolation. The accuracy of the registration methods was assessed by the coincidence between the individuals' registered

organs and the template. Although many metrics exist to evaluate this similarity [10], we only used the *Dice Score*, defined as:

$$Dice = \frac{2|A \cap B|}{|A| + |B|}$$

where $| \cdot |$ indicates the number of voxels of the considered A and B volumes. In that way, the *Dice Score* will range between 0 and 1, depending on the overlap.

3. Results

Fig. 2 shows some visual results of overlap between the prostate on the template (white) and the registered individual (red), for the different registration methods. In Fig. 3, checker-board views between the template (white) and an image before registration, after a RMA registration and after a FFD registration allows to visually assess the performances. On these figures, we can see that the prostate overlap (Fig. 2), and the correspondence between the images were better obtained (for the skin and the bones) with the FFD registration.

Fig. 4 depicts the results of the comparison for all the organs and for the four registration methods. These results suggest that, among the four registration methods, the FFD provides the higher overlap with a median *Dice Score* of 0.61 for the prostate, 0.66 for the bladder and 0.54 for the rectum.

3.1. Affine registration

In Fig. 4, one can see that the results were improved by restricting the computation to the individual's body, discarding the background of the image. Both affine registration methods (BMA and RMA), are based on the same algorithm and used the same similarity measure.

3.2. Non-rigid registration

Fig. 4 shows that non-rigid registrations outperformed the affine methods. The FFD registration (ARM + FFD) provided better results for all the considered organs (median Dice Score greater than 0.6 for the prostate and the bladder), with a large variability, yet, mainly for the bladder. This result was expected as the bladder variability is higher across the individuals than the

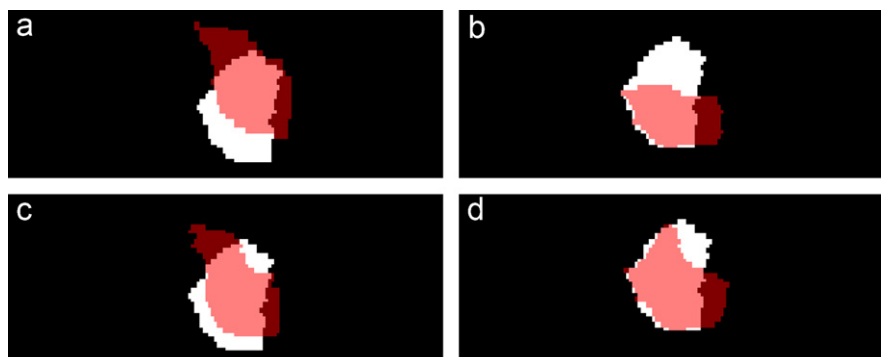


Fig. 2. Example of an individual's registered prostate (red) overlaid on the middle slice of the template's prostate (white) after a: (a) BMA, (b) RMA, (c) demons and (d) FFD registration.

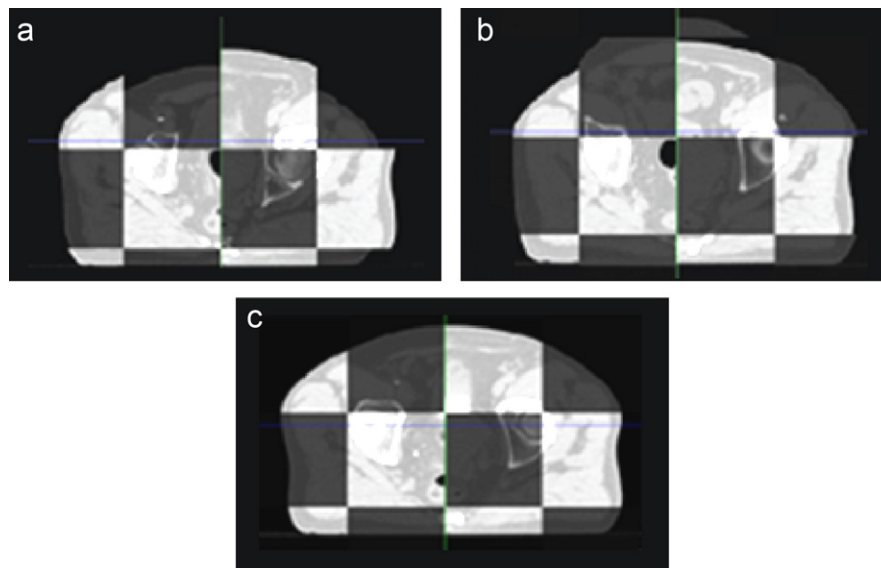


Fig. 3. Checkerboard views of a computed tomography (CT) template (white) and an individual's computed tomography (a) before registration, (b) after a restricted block matching (RMA) registration and (c) after a free-form deformation (FFD) registration (dark gray).

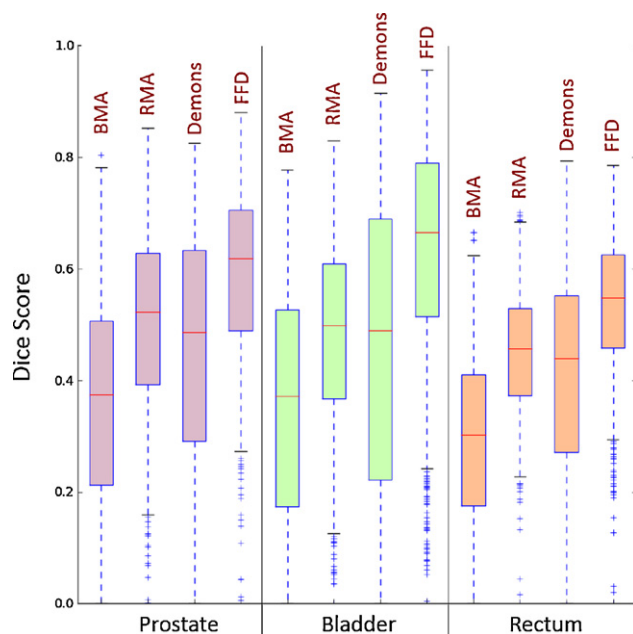


Fig. 4. Dice scores obtained with the four registration strategies block matching (BMA), restricted block matching (RMA), demons and free-form deformation (FFD).

rectum and bladder. Results show also that ARM + FFD provides better results than the demons registration (BMA + demons).

4. Conclusion

We presented in this paper a quantitative comparison of four intensity-based registration strategies for the alignment of inter-individual pelvic CT. Results showed that non-rigid registration algorithms performed better in the mapping of prostate, bladder and rectum. However, those methods relying only on the CT gray-level intensities lack of informations to accurately register

those organs for performing voxel-wise population analysis. In this paper, we brought up the issues related with the mapping of organs where the contrast is poor and there is a lack of gradient between soft tissues. With the considered registration methods, the main organs of interest, namely prostate, bladder and rectum, just follow the deformation imposed by more visible structures in the CT images, such as the bones and the skin. Future works implementing a hybrid non-rigid registration strategy, driven by the organ segmentations may be a promising solution for the mapping of structures of interest.

Disclosure of interest

The authors declare that they have no conflicts of interest concerning this article.

References

- [1] Fitzpatrick JM. The role of registration in accurate surgical guidance. *Proc Inst Mech Eng [H]* 2010;224:607–22.
- [2] Castadot P, Lee JA, et al. Comparison of 12 deformable registration strategies in adaptive radiation therapy for the treatment of head and neck tumors. *Radiat Oncol* 2008;89(1):1–12.
- [3] Ashburner J, Friston KJ. Nonlinear spatial normalization using Bbasis functions. *Hum Brain Mapp* 1999;7:254–66.
- [4] Park H, Meyer CR, et al. Validation of automatic target volume definition as demonstrated for 11c-choline pet/ct of human prostate cancer using multimodality fusion techniques. *Acad Radiol* 2010;17(5):614–23.
- [5] Chételat G, Desgranges B, et al. Direct voxel-based comparison between grey matter hypometabolism and atrophy in alzheimer's disease. *Brain* 2007;131(1):60–71.
- [6] Rohlfing T, Sullivan EV, et al. Subject-matched templates for spatial normalization. *Miccai'09* 2009;12(Pt 2):224–31.
- [7] Lu C, Chelikani S, et al. Integrated segmentation and non-rigid registration for application in prostate image-guided radiotherapy. *Miccai'10*. Berlin: Heidelberg; 2010, p. 53–60.
- [8] Acosta O, Simon A, et al. Evaluation of multi-atlas-based segmentation of CT-scans in prostate cancer radiotherapy. *IEEE ISBI*. 2011, p. 1966–9.

- [9] Aljabar P, Heckemann RA, et al. Multi-atlas based segmentation of brain images: atlas selection and its effect on accuracy. *Neuroimage* 2009;46:726–38.
- [10] Klein A, Andersson J, et al. Evaluation of 14 nonlinear deformation algorithms applied to human brain MRI registration. *Neuroimage* 2009;46(3):786–802.
- [12] Kaus MR, Brock KK, et al. Assessment of a model-based deformable image registration approach for radiation therapy planning. *Int J Radiat Oncol Biol Phys* 2007;68(2):572–80.
- [13] Zhong H, Peters T, et al. Fem-based evaluation of deformable image registration for radiation therapy. *Phys Med Biol* 2007;52(16):4721–38.
- [14] Acosta O, Dowling J, et al. Atlas-based segmentation and mapping of organs at risk from planning ct for the development of voxel-wise predictive models of toxicity in prostate radiotherapy. *Prostate Cancer Imaging. Miccai'10*, volume 6367 of LNCS, 42–51. Springer Berlin: Heidelberg; 2010.
- [15] Wang H, Dong L, et al. Implementation and validation of a three-dimensional deformable registration algorithm for targeted prostate cancer radiotherapy. *Int J Radiat Oncol Biol Phys* 2005;61(3):725–35.
- [16] Shen J-K, Matuszewski BJ, et al. Deformable image registration - a critical evaluation: Demons b-spline ffd and spring mass system. 2008.
- [17] Ourselin S, Roche A, et al. Reconstructing a 3d structure from serial histological sections. *Image Vision Comput* 2001;19(1–2):25–31.
- [18] Thirion J-P. Image matching as a diffusion process: an analogy with Maxwell's demons. *Med Image Analysis* 1998;2(3):243–60.
- [19] Vercauteren T, Pennec X, et al. Non-parametric diffeomorphic image registration with the demons algorithm. *Miccai'07* 2007;4792/2007:319–26.
- [20] Rueckert D, Sonoda LI, et al. Non-rigid registration using free-form deformations: application to breast MRI images. *IEEE transactions on Med. Imaging* 1999;18:712–21.
- [21] Modat M, Ridgway GR, et al. Fast free-form deformation using graphics processing units. *HP-MICCAI'08* 2010;98:278–84.
- [22] Heemsbergen WD, et al. Urinary obstruction in prostate cancer patients from the dutch trial (68 gy vs. 78 gy): relationships with local dose, acute effects, and baseline characteristics. *Int J Radiat Oncol Biol Phys* 2010;78:19–25.
- [23] Witte MG, et al. Relating dose outside the prostate with freedom from failure in the dutch trial 68 gy vs. 78 gy. *Int J Radiat Oncol Biol Phys* 2010;77:1131–8.